In-Situ Raman Spectroscopy to Study Supercritical Water Gasification of Formic Acid

Brian Pinkard, David Gorman, Kartik Tiwari, Justin Davis, Elisabeth Rasmussen, John Kramlich, Per Reinhall, Igor Novosselov*
Mechanical Engineering Department, University of Washington; Seattle, WA, USA 98466
* Corresponding author e-mail: ivn@uw.edu

ABSTRACT

Supercritical water gasification (SCWG) is an emerging technology with applications in renewable energy and waste processing. Environmentally benign, SCWG relies on supercritical water to decompose organic molecules. A continuous supercritical water reactor with high-resolution *in-situ* Raman spectroscopy was designed and fabricated, enabling real-time process monitoring. This reactor was used to study gasification of formic acid at temperatures between 300 and 400°C, at a constant pressure of 25 MPa, at residence times between 8.7 and 39 s, and at a constant feedstock concentration of 6.1 wt%. *In-situ* Raman spectroscopy significantly reduced experimental uncertainty and experimentation time, while allowing for the accurate identification of formic acid decomposition products, namely H_2, CO_2, and trace amounts of CO. Collected spectra can be used for the quantification of decomposition kinetics.

INTRODUCTION

SCWG is a promising technology to produce fuel gas from wet biomass and to treat chemical and biological waste. Above its critical point (374°C, 22.1 MPa), water becomes a useful reaction medium, as the physical and chemical properties of water change significantly. The dielectric constant of water decreases across the critical point, and hydrogen bonds become less prevalent, drastically changing the solubility of various materials. Salts, such as NaOH and KOH, become insoluble, while organic molecules become soluble and decompose in the high-temperature, high-pressure (HTHP) hydrolysis environment [1].

In pursuit of advancing SCWG technology towards large-scale applications, researchers have extensively studied gasification chemistry in both continuous-flow and batch supercritical water reactors. Both system types have been used to obtain valuable experimental data, however, continuous-flow reactors offer several benefits over batch reactors both as research tools and industrial systems. Flow-through operation allows for continuous tuning of process parameters, decreased experimentation time, and increased process efficiency. In industrial applications, the continuous process allows for high throughput, operational flexibility, real time process monitoring and control, and efficient operation. A high surface-to-volume ratio in a flow-through system offers another significant benefit: the nickel walls of the reactor can act as a catalytic surface for enhancing chemical kinetic rates [2].

Basic knowledge of decomposition rates for target compounds is required to advance SCWG science and engineering for large-scale applications. Researchers have long sought to fully characterize chemical reaction mechanisms in the gasification environment. Reaction pathways and compound decomposition rates have been proposed for several model compounds, such as glucose, phenol, benzene, and methanol [2]. The behavior of intermediate compounds from the decomposition of these model compounds is largely unknown but is necessary for the development of a robust chemical kinetic model. Additionally, few of these kinetic rates have been cross-verified by subsequent studies, partly due to lengthy experimentation times. Gas chromatography [3 - 5] TOC analysis [6, 7], and other common *ex-situ* analytical methods are time-consuming, as the reactor conditions can only be changed from run-to-run.

Alternatively, *in-situ* process monitoring makes it possible to identify gasification products in real time and to change operational parameters rapidly. In this work, *in-situ* Raman spectroscopy is used to directly monitor species concentration in the effluent stream, decreasing experimentation time and reducing

measurement uncertainty.

Previous studies have investigated the viability of using Raman spectroscopy in the HTHP environment, with limited success. Raman spectroscopy is well suited to HTHP processes; other spectroscopic techniques, e.g. IR spectroscopy, have limited application due to the broad absorption spectra of water. Hunter, Rice, and Hanush at Sandia National Laboratories [8 - 10] demonstrated the capability of *in-situ* Raman spectroscopy to monitor intermediate products in real time by studying the oxidation of methanol and isopropyl alcohol in supercritical water. However, long term use of the spectroscopic cell proved to be a challenge. A sapphire or diamond window is necessary for optical access to the flow due to the corrosive nature of supercritical water. In the HTHP environment, it is challenging to keep the window sealed and intact. Thermal expansion of surrounding materials can cause the window to fracture, and gaskets (typically gold or graphite) deform and creep due to thermal cycling [11].

Nearly all continuous-flow supercritical water reactors have been constructed using materials with high nickel content, which provide excellent corrosion resistance and beneficial catalytic activity at the reactor wall. Batch reactors can be constructed from quartz or similar non-catalytic materials, but these materials are expensive and difficult to work with. The walls of continuous-flow reactors must withstand high pressure and temperature as well as the corrosive nature of supercritical water and reaction products. DiLeo and Savage [12] gasified methanol at supercritical conditions in quartz capillary batch reactors, both absent of and in the presence of, a wire nickel rod. The nickel caused decomposition to occur roughly 100 times faster. For scale-up to industrial applications, this catalytic behavior is beneficial to overall system throughput and efficiency.

Though the catalytic effect of nickel in the reactor walls in continuous flow reactors is a known phenomenon, it has not been quantified for various reactor geometries, which complicates comparisons between studies. Variations in the surface-to-volume ratio are expected to result in different chemical reaction rates between similar reactors. Goodwin and Rorrer [3] showed that a microchannel reactor increased the speed of gasification reactions, due to smaller inner reactor geometries. Hao et al. [5] also demonstrated that smaller inner reactor diameters are beneficial for gasification, as they increase reactor surface-to-volume ratio. Reactors constructed from materials with different nickel contents (i.e. Inconel 625 vs. 316 SS) are expected to show different catalytic behavior. For accurate studies of chemical kinetic rates in continuous-flow supercritical water reactors, the exact reactor geometries and materials must be specified, and the catalytic effects of the reactor wall should be considered. The presence of the catalytic surface may affect product yields, reaction pathways, and elemental rates.

In the gasification of model organic compounds, some intermediate reaction products are common across a range of compound types. One of these common intermediate reaction products is formic acid; it has been explicitly listed as an intermediate compound from the gasification of glucose [3], fructose [4], methanol [13], and glycine [14]. Because formic acid is present in the gasification pathways of model carbohydrates, alcohols, and amino acids, one can assume that formic acid will be present during the gasification of any real biomass feedstock.

In 1998, Yu and Savage [15] studied the gasification of dilute formic acid in a continuous-flow, supercritical water reactor, to analyze the decomposition pathways and rates under hydrothermal conditions. An aqueous feedstock was used, with 1000 ppm formic acid in distilled, deionized water. Arrhenius parameters were determined, and the preferred reaction pathway was identified. Tests were conducted at temperatures between 320 and 500°C, pressures between 18 and 30.7 MPa, and residence times between 1.4 and 80 s. Major decomposition products were consistently CO_2 and H_2, indicating that decarboxylation was the dominant reaction pathway, as shown in Equation 1. CO was also observed as a reaction product in low concentrations, indicating the existence of a dehydration reaction pathway, which occurs as indicated in Equation 2.

$$HCOOH \rightarrow H_2 + CO_2 \quad (1)$$

$$HCOOH \rightarrow H_2O + CO \quad (2)$$

For temperatures above 420°C, decomposition happened too rapidly for kinetic rates to be properly determined. Some pressure dependency was noted for decomposition occurring near the critical point, which may indicate a density-dependent reaction mechanism, as the density of water changes drastically with changing pressure near the critical point. Kinetic parameters were calculated for temperatures from 320 to 420°C and a pressure of 25.3 MPa. First-order decomposition behavior was observed, and Arrhenius parameters are presented in Table 1.

In a more recent study, Zhang et al. [16] gasified formic acid in a continuous-flow reactor, at temperatures between 550 and 650°C pressures between 24 and 30 MPa, and residence times between 16 and 46 s. Concentrations between 0.05 and 0.7 M of formic acid in distilled, deionized water were tested. Dominant reaction products were reported as H_2 and CO_2, with minor yields of CO, again supporting the conclusion that decarboxylation is the dominant reaction mechanism at supercritical conditions. The authors reported that gasification with a high concentration of formic acid led to side-reactions involving the formation of formaldehyde and methanol, decreasing hydrogen yield. Kinetic rates were not reported.

Table 1: Arrhenius parameters of first-order formic acid decomposition

Decomposition Reaction	Temperature Range (°C)	Pressure (MPa)	Pre-Exponential Factor 'A' (s^{-1})	Activation Energy 'E_A' (kJ/mol)	Source
Formic Acid	320 - 420	25.3	6.2	85.77	[15]

In this study, formic acid gasification was studied at temperatures between 300 and 400°C, at a constant pressure of 25 MPa, and at residence times between 8.7 and 39 s. The initial concentration of formic acid was maintained at 6.1 wt%. *In-situ* process monitoring with Raman spectroscopy allowed for analysis of the decomposition process. The use of Raman spectroscopy was demonstrated for continuous process monitoring and species identification. The potential for determining chemical kinetic rates is discussed in the context of the results obtained.

MATERIALS AND METHODS

The reactor used for this study is designed to operate at pressures up to 35 MPa, temperatures up to 650°C, residence times of 0.7 – 70 s, and a maximum throughput of 41 g of H_2O per minute. A system schematic is shown in Figure 1. The reactor components are Inconel 625, a nickel alloy with excellent corrosion resistance and strength at elevated temperatures. This is similar to SCWRs reported in the literature, which are primarily constructed from high nickel alloys such as Inconel 625 or Hastelloy C-276 [2-7]. The reactor is constructed of 6.35 mm (0.25 in) tubing with an internal diameter of 3.05 mm (0.120 in), giving a surface to volume ratio of 13.1 cm^{-1}. A modular reactor design allows the reactor section to vary in length, volume, and material of the reactor. Two different reactor sections may be installed on the system; both are Inconel 625 tubing, with varied length to provide a greater range of residence times. The first reactor section has an internal volume of 17.4 mL and can achieve residence times of 1.8 to 74 s (based on water density at 600°C). The second reactor section has an internal volume of 6.25 mL and can achieve residence times of 0.65 to 27 s (at 600°C). The insulated reactor section is followed by a Graham Heliflow tube-in-shell heat exchanger designed to rapidly cool the fluid, quenching any ongoing high-temperature reactions. The time required to cool the effluent flow to a temperature at which decomposition is no longer occurring was not precisely determined but is assumed to be less than one second. In this study the reaction rates are not calculated, thus any uncertainties in residence time calculations arising from effluent cooling are not of critical importance. However, for future studies, this correction in residence time should be considered.

Two SSI HPLC pumps provide a constant, user-defined flow rate of reagent and water into the system, while an Equilibar diaphragm-style back pressure regulator controls the internal reactor pressure. To bring the water to supercritical conditions, two separate heating sections are employed. The first heater consists of a 2000 W TEMPCO coil-heater. This heater is in direct contact with a 19.0 mm (0.75 in) tube with an internal

diameter of 13.0 mm (0.51 in). To reach supercritical temperatures, an 1800 W OMEGA ceramic radiant cylinder heater provides heat into a coiled section of 6.35 mm (0.25 in) tubing.

A custom mixing section was designed and fabricated to ensure rapid mixing and heating of the reactant stream. The mixing technique was carefully considered in the reactor design. Some researchers choose to premix reactant and water, to simplify pumping the feedstock and the overall plumbing of the system. This may be desirable for large-scale systems with non-ideal feedstocks, but premixing is not ideal for chemical kinetic studies. Heating a premixed effluent leads to slow heating of the reactant, which can cause decomposition and polymerization to begin before the desired temperature is reached [4]. As an alternative, post-critical injection is attractive for rate studies, as it can achieve nearly instantaneous heating of the reactant at low concentrations, limiting polymerization and char formation. Also, mixing cool reactant into supercritical water establishes a clear initiation point for chemical reactions, which is necessary for accurate residence time calculations. Post-critical injection does not guarantee a well-mixed flow or a uniform temperature distribution, as laminar flow can lead to slow mixing between the supercritical water and reactants. Additional analysis is necessary to assess the mixing and temperature distribution. A numerical computational fluid dynamic (CFD) study was performed to design a suitable mixing section to improve mixing in the laminar and transitional (to turbulence) flow regions in the reactor; this process is detailed in Tiwari et al. [17].

After the mixing section, a 700 W OMEGA radiant cylinder heater is used to ensure the decomposition reaction takes place under isothermal conditions. The heater was placed around the coiled Inconel reactor section. A Raman immersion ball probe from MarqMetrix was installed immediately after the heat exchanger and prior to the back pressure regulator, to allow for *in-situ* monitoring of product species concentrations. The Raman spectroscopic cell was positioned in the cold flow region after the heat exchanger to avoid the thermal expansion and sealing issues described above. Two Honeywell Model S flush mount pressure transducers are used to monitor internal pressure one immediately after the pumps and one after the heat exchanger. OMEGA type-K thermocouples monitor flow temperature at the mixing section, reactor inlet and outlet, and the Raman probe.

The fiber-optic Raman laser has an excitation wavelength of 785 nm and was operated at 300 mW. A sapphire ball lens is used to focus the excitation light 0.6 mm in front of the lens. The ball lens protrudes 0.5 mm into the flow. Spectra were collected in the backscatter configuration where the exciting laser and the collected spectra enter and exit the measurement volume through the same optical window, and along the same axis. To achieve consistent signals and to reduce measurement uncertainty, 20 to 40 averages of the signal were collected, with a signal integration time of 0.5 to 1 s. This reduced signal noise and ensured that

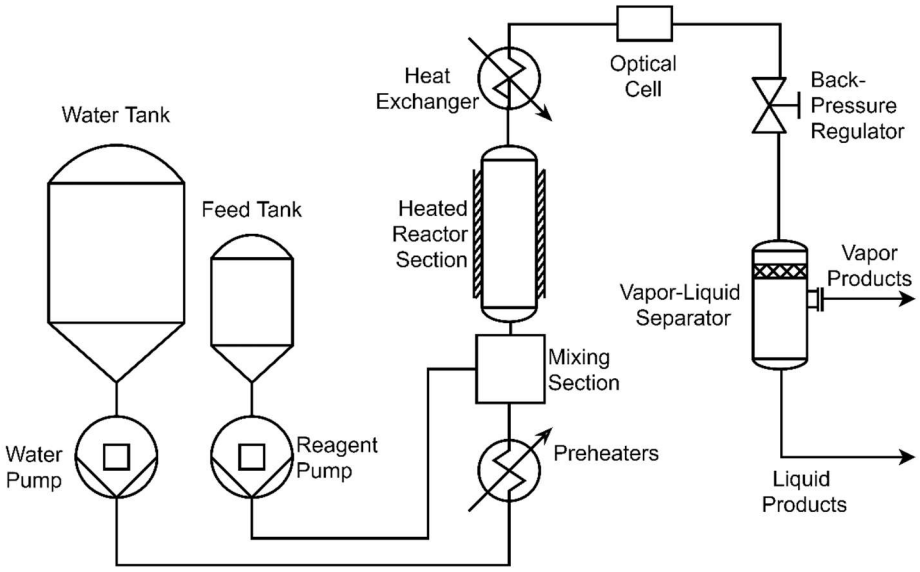

Figure 1. Schematic of the UW reactor system. The system can operate at pressures up to 35 MPa and temperatures up to 650°C, with residence times of 0.7 – 70 s. The maximum throughput of the system is 41 g of H_2O per minute.

minor signal constituents were collected accurately. Variations in integration time leads to a linear difference in signal magnitude; the data were corrected in post-processing to account for different integration times for each experiment. The fluorescent background signal was subtracted manually using Origin 2018 software.

RESULTS

Formic acid was gasified in this continuous-flow reactor at temperatures of 300°C, 350°C, 374°C, 387°C, and 400°C, at a constant pressure of 25 MPa, and at residence times between 8.7 and 39 s. Feedstock concentration was held fixed at 6.1 wt% and total mass flow rate was kept constant at 20.4 g/min. Gasification resulted in decomposition into CO_2, H_2, and trace amounts of CO. Monitoring the gasification reaction with Raman spectroscopy proved to be an effective *in-situ* technique for identifying reaction products. Multiple spectra were gathered for each individual set of experimental parameters and no significant differences were observed between the spectra. This ensured that for each experiment, the chemical composition within the optical volume of the laser had reached steady state prior to acquiring the spectra.

Table 2 lists compounds present in the Raman spectra and associated wavenumbers of significant peaks. These peaks may be slightly shifted from the reference data provided by several Raman libraries due to differences in operating temperature or pressure. Figure 2 shows the Raman spectra of the decomposition products formed from gasifying formic acid at 374°C. The corresponding wavenumbers of significant peaks are noted on the plot. This temperature is chosen because it clearly contains all Raman peaks observed in the experiments.

Table 2. Compounds present in Raman spectra of the product stream, with locations of Raman peaks noted

Compound	Wavenumbers of Significant Raman Peaks (cm^{-1})
Sapphire (Al_2O_3)	379, 418, 751
Water (H_2O)	1640, 3185
Formic Acid (HCOOH)	712, 1219, 1400, 1714, 2943
Hydrogen (H_2)	355, 587, 814, 1034
Carbon Dioxide (CO_2)	1272, 1383
Carbon Monoxide (CO)	2138

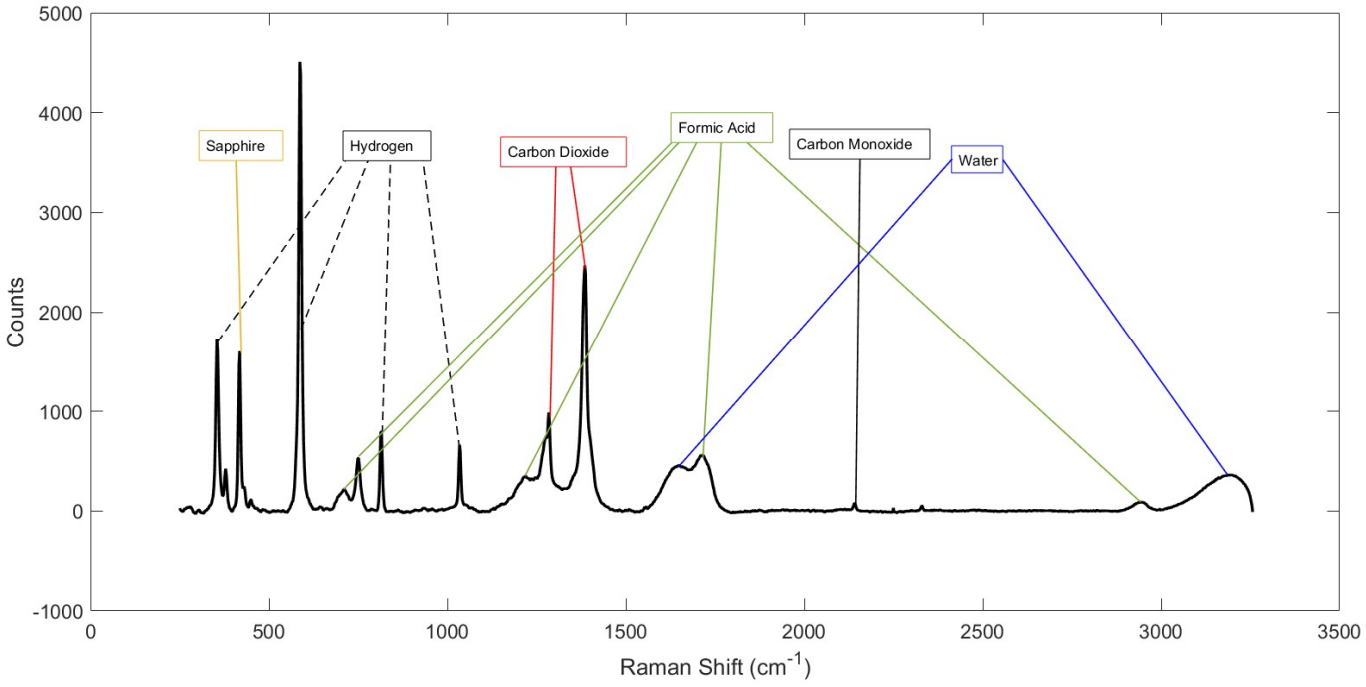

Figure 2. Raman spectra of decomposition products of formic acid at 374°C, with significant Raman spikes identified by correlated chemical species.

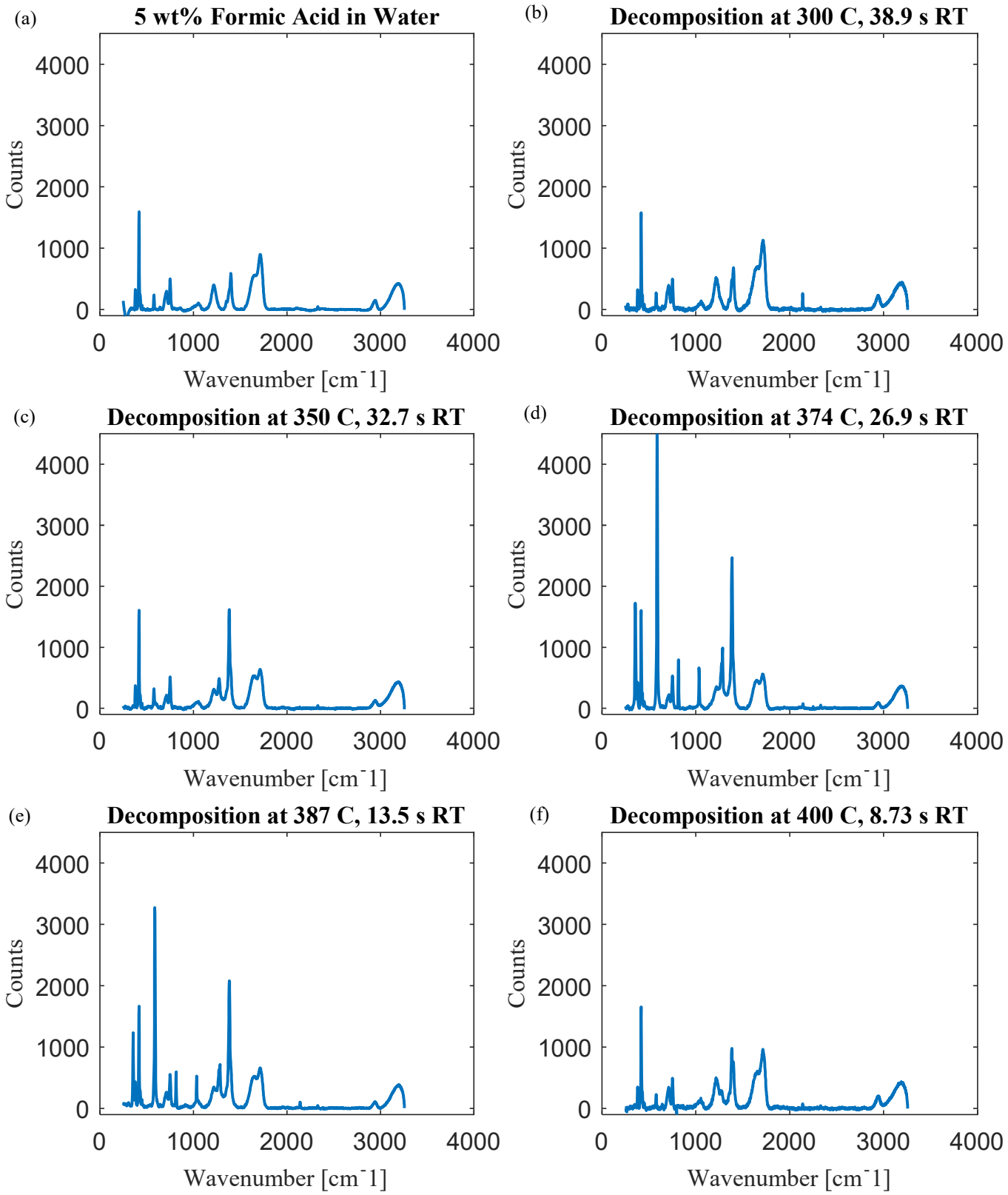

Figure 3. Raman spectra of (a) formic acid and (b) – (f) its decomposition products at tested temperatures and residence times. Spectrum (b) shows decomposition at 300°C, where only a small amount of CO_2 and CO can be observed. Spectra (c) – (f) show increased yields of H_2 and CO_2, as reaction temperatures are increased.

The full decomposition behavior is shown in Figure 3. The baseline signal of 6.1 wt% formic acid dissolved in deionized water is shown in Figure 3(a) for comparison to spectra of decomposition products. Each decomposition test was performed with a total mass flow rate of 20 mL/min through the reactor, which resulted in different residence times for each test due to lower densities at higher temperatures. At 300°C (b) and a residence time of 38.9 s, hardly any decomposition is observed, although small peaks associated with CO and CO_2 are visible. At higher temperatures of 350°C (c), 374°C (d), and 387°C (e), with residence times of 32.7, 26.9, and 13.5 s respectively, higher concentrations of H_2 and CO_2 are clearly visible in the product spectra. Formic acid peaks also appear to be diminishing in relation to peaks correlated with these gaseous products. Decomposition at 400°C (f) and a residence time of 8.73 s shows less decomposition than lower temperature tests, likely due to the shorter residence time. Future experiments will monitor decomposition at a range of residence times for each reaction temperature, to allow for the calculation of kinetic rates and Arrhenius parameters of the decomposition reactions. Concentration measurements are required for these calculations; a robust method for translating Raman spectra into concentration data is currently being developed.

To generalize the process of monitoring decomposition and identifying intermediate products with Raman spectroscopy, it is necessary to develop a library of potential reaction intermediates and products. From this study, the Raman spectra of formic acid, H_2, CO_2, CO, sapphire, and water are known, but future studies involving more complex decomposition pathways will require the methodical identification of Raman spectra of intermediate species. This will be accomplished by sequentially gasifying increasingly complex molecules. Subsequent experiments will be performed with gasification of acetic acid, methanol, and ethanol.

CONCLUSION

In this study, formic acid gasification in a continuous supercritical water reactor was studied at temperatures between 300 and 400°C, a pressure of 25 MPa, residence times between 8.7 and 39 s, and a feedstock concentration of 6.1 wt%. The feasibility of monitoring the gasification process with high-resolution Raman spectroscopy was demonstrated. Reaction products were identified as H_2, CO_2, CO, and residual formic acid from known Raman peaks observed in collected spectra. At temperatures below 300°C formic acid does not show any significant decomposition.

Supercritical water gasification is a promising technology for the destruction of waste products and the production of useful compounds and fuels. Temperature, residence time, and feedstock concentrations are the most relevant parameters in determining decomposition routes and rates. Additional work is required to determine the decomposition pathways and intermediate products for a broader set of operating conditions and for more complex organic model compounds. In future studies kinetic rates and Arrhenius parameters of observed decomposition reactions will be calculated; concentration data will be extracted from Raman spectra. Future research should consider the effects of reactor geometry, mixing and heating profiles, operating conditions, and potential catalytic activity of the walls. A more complete characterization of model compound decomposition rates in the SCWG environment can lead to a robust chemical reaction model to aid in the design and operation of supercritical water reactors for industrial applications.

ACKNOWLEDGMENTS

The authors would like to recognize the funding provided by the DOD Defense Threats Reduction Agency – Grant HDTRA1-17-1-0001, as well as the resources provided by the University of Washington which made this work possible.

REFERENCES

1. KRUSE A., Supercritical water gasification, Biofuels, Bioproducts and Biorefining, 2, 2008, p. 415.
2. PINKARD B., GORMAN D., TIWARI K., KRAMLICH J., REINHALL P., NOVOSSELOV I., Review of Gasification of Organic Compounds in Continuous-Flow, Supercritical Water Reactors, Industrial & Engineering Chemistry Research, 57, 2018, p. 3471.

3. GOODWIN A., RORRER G., Conversion of Glucose to Hydrogen-Rich Gas by Supercritical Water in a Microchannel Reactor, Industrial & Engineering Chemistry Research, 47, 2008, p. 4106.
4. KABYEMELA B., ADSCHIRI T., MALALUAN R., ARAI K., Glucose and Fructose Decomposition in Subcritical and Supercritical Water: Detailed Reaction Pathway, Mechanisms, and Kinetics, Industrial & Engineering Chemistry Research, 38, 1999, p. 2888.
5. HAO X., GUO L., MAO X., ZHANG X., CHEN X., Hydrogen Production from Glucose used as a Model Compound of Biomass Gasified in Supercritical Water, International Journal of Hydrogen Energy, 28, 2003, p. 55.
6. CAPUTO G., RUBIO P., SCARGIALI F., MAROTTA G., BRUCATO A., Experimental and Fluid Dynamic Study of Continuous Supercritical Water Gasification of Glucose, The Journal of Supercritical Fluids, 107, 2016, p. 450.
7. AIDA T., TAJIMA K., WATANABE M., SAITO Y., KURODA K., NONAKA T., HATTORI H., SMITH JR. R., ARAI K., Reactions of D-Fructose in Water at Temperatures up to 400 C and Pressures up to 100 MPa, The Journal of Supercritical Fluids, 42, 2007, p. 110.
8. HANUSH R., TICE S., HUNTER T., AIKEN J., Operation and Performance of the Supercritical Fluids Reactor (SFR), Sandia National Laboratories: Livermore, CA, 1995.
9. RICE S., HUNTER T., RYDEN, Å., HANUSH, R., Raman spectroscopic measurement of oxidation in supercritical water. 1. Conversion of methanol to formaldehyde, Industrial & Engineering Chemistry Research, 35, 1996, p. 2161.
10. HUNTER T., RICE S., HANUSH R., Raman spectroscopic measurement of oxidation in supercritical water. 2. Conversion of isopropyl alcohol to acetone, Industrial & Engineering Chemistry Research, 35, 1996, p. 3984.
11. RICE S., STEEPER R., LAJEUNESSE C., HANUSH R., AIKEN J., Design strategies for high-temperature, high-pressure optical cells, Sandia National Laboratories: Livermore, CA, 1997.
12. DILEO G., SAVAGE P., Catalysis during methanol gasification in supercritical water, The Journal of Supercritical Fluids, 39, 2006, p. 228.
13. HACK W., MASTEN D., BUELOW S., Methanol and ethanol decomposition in supercritical water, Zeitschrift für Physikalische Chemie, 219, 2005, p. 367.
14. SATO N., DAIMON H., FUJIE K., Decomposition of Glycine in High Temperature and High Pressure Water, Kagaku Kogaku Ronbunshu, 28, 2002, p. 113.
15. YU J., SAVAGE P., Decomposition of Formic Acid under Hydrothermal Conditions, Industrial & Engineering Chemistry Research, 37, 1998, p. 2.
16. ZHANG Y., ZHANG J., ZHAO L., SHENG C., Decomposition of Formic Acid in Supercritical Water, Energy & Fuels, 24, 2010, p. 95.
17. TIWARI K., PINKARD B., GORMAN D., DAVIS J., KRAMLICH J., REINHALL P., NOVOSSELOV I., Computational Modeling of Mixing and Gasification in Continuous-Flow Supercritical Water Reactor, Proceedings of 12th International Symposium on Supercritical Fluids, 2018.